

ARTICLE

Open Access

Midostaurin potentiates rituximab antitumor activity in Burkitt's lymphoma by inducing apoptosis

Xiaowen Ge¹, Jianfeng Chen², Ling Li², Peipei Ding², Qi Wang², Wei Zhang², Luying Li², Xinyue Lv², Danlei Zhou², Zhengzeng Jiang¹, Haiying Zeng¹, Yifan Xu¹, Yingyong Hou¹ and Weiguo Hu^{1,2} 

Abstract

An intensive short-term chemotherapy regimen has substantially prolonged the overall survival of Burkitt's lymphoma (BL) patients, which has been further improved by addition of rituximab. However, the inevitable development of resistance to rituximab and the toxicity of chemotherapy remain obstacles. We first prepared two BL cell lines resistant to rituximab-mediated CDC. Using a phosphorylation antibody microarray, we revealed that PI3K/AKT pathway contained the most phosphorylated proteins/hits, while apoptosis pathway that may be regulated by PKC displayed the greatest fold enrichment in the resistant cells. The PI3K/AKT inhibitor IPI-145 failed to reverse the resistance. In contrast, the pan-PKC inhibitor midostaurin exhibited potent antitumor activity in both original and resistant cells, alone or in combination with rituximab. Notably, midostaurin promoted apoptosis by reducing the phosphorylation of PKC and consequently of downstream Bad, Bcl-2 and NF- κ B. Therefore, midostaurin improved rituximab activity by supplementing pro-apoptotic effects. In vivo, midostaurin alone powerfully prolonged the survival of mice bearing the resistant BL cells compared to rituximab alone treatments. Addition of midostaurin to rituximab led to dramatically improved survival compared to rituximab but not midostaurin monotherapy. Our findings call for further evaluation of midostaurin alone or in combination with rituximab in treating resistant BL in particular.

Introduction

Burkitt's lymphoma (BL), a highly aggressive non-Hodgkin's B-cell lymphoma, accounts for 3–5% of lymphoma cases in all age groups and 40–50% of all childhood lymphomas¹. Adult BL patients have shown a poor response to a CHOP (cyclophosphamide, doxorubicin, vincristine and prednisolone)-based regimen, with 2-year and 5-year overall survival (OS) rates of approximately 50–65%, decreasing to less than 30% with bone marrow or central nervous system involvement^{2,3}. In contrast, an

intensive short-term chemotherapy regimen has substantially improved the survival rates to greater than 90% in childhood BL patients^{4,5}. Similar regimens in adult BL patients have achieved advances in outcomes, with OS rates exceeding 70%^{6–9}. Despite the success of these regimens, further progress is required to achieve a therapeutic strategy that can reduce toxicity and overcome drug resistance in currently incurable patients.

The combination of rituximab with CHOP chemotherapy (R-CHOP) has improved overall survival by at least 20% in cases of diffuse large B-cell lymphoma (DLBCL)¹⁰. Similarly, many single-arm clinical trials have confirmed the effect of adding rituximab to the intensive short-term chemotherapy regimens for BL^{11–15}. A recent phase III clinical trial has shown that addition of rituximab to chemotherapy achieved better 3-year event-free survival (75% vs 62%, $P = 0.024$) and 3-year OS (83% vs

Correspondence: Yingyong Hou (hou.yingyong@zs-hospital.sh.cn) or Weiguo Hu (weiguohu@fudan.edu.cn)

¹Department of Pathology, Zhongshan Hospital, Fudan University, Shanghai, China

²Fudan University Shanghai Cancer Center and Institutes of Biomedical Sciences; Shanghai Medical College, Fudan University, Shanghai 200032, China
These authors contributed equally to this work: Xiaowen Ge, Jianfeng Chen.
Edited by M. Diederich

© The Author(s) 2018



Open Access This article is licensed under a Creative Commons Attribution 4.0 International License, which permits use, sharing, adaptation, distribution and reproduction in any medium or format, as long as you give appropriate credit to the original author(s) and the source, provide a link to the Creative Commons license, and indicate if changes were made. The images or other third party material in this article are included in the article's Creative Commons license, unless indicated otherwise in a credit line to the material. If material is not included in the article's Creative Commons license and your intended use is not permitted by statutory regulation or exceeds the permitted use, you will need to obtain permission directly from the copyright holder. To view a copy of this license, visit <http://creativecommons.org/licenses/by/4.0/>.

70%, $P=0.011$) rates than chemotherapy alone¹⁶. Therefore, addition of rituximab is highly anticipated in the future design of anti-BL regimens, and the subsequent development of resistance to rituximab may be predictable as it has occurred in DLBCL¹⁷.

By binding to the membrane protein CD20, rituximab destroys lymphocytes mainly via antibody-dependent cellular cytotoxicity (ADCC) and complement-dependent cytotoxicity (CDC)^{17–19}. The resistance to ADCC probably results from the intrinsic polymorphism of the IgG Fc receptor *FcγRIIIa* gene²⁰, whereas the resistance to CDC can most likely be attributed to the down-regulation of CD20 expression and the elevated expression of membrane complement regulatory proteins (mCRPs), especially CD59 expression^{17,21,22}. However, many studies have revealed that rituximab fails to induce apoptosis to any detectable extent in B-cell lymphoma, including in BL cells^{23–30}. Therefore, the development of a pro-apoptotic agent to combine with rituximab is a rational approach to achieving either high anti-cancer efficacy with rituximab or overcoming the resistance to rituximab. To identify such an alternative therapeutic approach, we prepared two BL cell lines resistant to rituximab-mediated CDC, interrogated the signaling pathways related to the development of resistance, and evaluated the effect of pathway inhibitors on antitumor activity and overcoming resistance.

Materials and methods

Cell culture and reagents

Two BL cell lines, Raji and Ramos, were purchased from American Type Culture Collection (Manassas, VA) and were maintained in RPMI-1640 medium supplemented with 10% fetal bovine serum (GIBCO BRL, Grand Island, NY) and 1% penicillin/streptomycin (Ambion, Austin, TX).

As a complement resource, normal human serum (NHS) was pooled from 10 healthy persons, aliquoted and stored at -80°C until use. The phosphoinositide 3-kinase (PI3K) inhibitor IPI-145³¹ and the protein kinase C (PKC) inhibitor midostaurin were purchased from Selleck Chemicals (Houston, TX), and dissolved in dimethyl sulfoxide (DMSO) in use. Consequently, same volume DMSO was used as control.

Generation of rituximab-resistant BL cells

We developed Raji and Ramos cells that were resistant to rituximab-mediated CDC as previously described³². Briefly, the original Raji or Ramos cells were treated with escalating rituximab (Roche, Basel, Switzerland) concentrations from 4 or 40 $\mu\text{g}/\text{mL}$ to 32 or 640 $\mu\text{g}/\text{mL}$, respectively, in the presence of 20% NHS. The resulting resistant cells were termed Raji32 and Ramos640, respectively. These cells were treated with 32 $\mu\text{g}/\text{mL}$ or

640 $\mu\text{g}/\text{mL}$ rituximab, respectively, and 20% NHS every 21 days to maintain resistance. The CDC effect was assessed by fluorescence-activated cell sorting (FACS) analysis to detect propidium iodide-positive cells.

Immunoblotting assay

We performed immunoblotting assays according to the standard protocol using the antibodies shown in Table S1.

FACS analysis

After washing with phosphate-buffered saline (PBS), cells were incubated with fluorescein-conjugated antibodies for 30 min and then rinsed and resuspended in PBS. Flow cytometric analysis was performed on a Cytomics FC500 MPL machine (Beckman Coulter, Brea, CA) and analyzed with the FlowJo software (Ashland, OR). We performed cell sorting with a MoFlo XDP instrument (Beckman Coulter, Brea, CA) based on fluorescence.

Apoptosis analysis was performed using the PE Annexin V Apoptosis Detection Kit (BD Pharmingen, San Diego, CA) according to the manufacturer's instructions.

CytoTox-Glo™ cytotoxicity assay

We used the CytoTox-Glo™ cytotoxicity assay kit (Promega, Madison, WI) to detect cytotoxicity. The cells were pretreated with rituximab and 20% NHS in the presence or absence of midostaurin for 48 h before assays. Cytotoxicity was calculated according to the formula: cytotoxicity (%) = dead cell luminescence/total luminescence $\times 100\%$.

Antibody microarray for profiling phosphorylation

Protein phosphorylation was profiled using a phosphorylation-profiling antibody microarray (Full Moon Microsystems, Catalog No. CSP100, Sunnyvale, CA) containing 269 antibodies against 131 protein phosphorylation sites; the procedure was performed by Wayen Biotechnology (Shanghai, China) according to the established protocol. Differentially phosphorylated proteins with a fold change >1.5 were screened by DAVID (Database for Annotation, Visualization and Integrated Discovery) to performed functional annotation³³. The interaction network among PKC subunits and the differentially phosphorylated proteins was analyzed using Ingenuity Pathway Analysis (IPA, QIAGEN, Dusseldorf, Germany).

RNA sequencing

RNA sequencing (RNA-seq) was performed as previously described³⁴. Briefly, total RNA was extracted and pooled separately from three different passages of Ramos and Ramos640 cells. The RNA quality was determined with a Bioanalyzer 2200 (Agilent Technologies, Santa,

Clara, CA). RNA with an RNA integrity number (RIN) >8.0 was considered acceptable for complementary DNA (cDNA) library construction. The RNA-seq was conducted by Shanghai Novellbio, Ltd. cDNA libraries were constructed using the Ion Total RNA-seq Kit v2.0 (Life Technologies, Gaithersburg, MD) and were then processed for RNA sequencing. Before the read mapping, clean reads were obtained from the raw reads by removing adaptor sequences, and these reads were then aligned to the human genome (version: GRCh37 NCBI) using the MapSplice program (v2.1.6). After the significance and false discovery rate (FDR) analyses were performed under the following criteria: (1) fold change >1.5 or <0.667 and (2) FDR <0.05, we applied the DEseq algorithm to filter the differentially expressed genes.

Gene set enrichment analysis

Using gene set enrichment analysis (GSEA) software (the Broad Institute at MIT), we performed a GSEA to identify the functions of the differentially expressed genes obtained from the RNA-seq^{35,36}. The pre-ranked version of the software was used to identify significantly enriched pathways, and enriched pathways with an FDR <0.25 were considered significant. The anti-apoptotic TNFs/NF- κ B/Bcl-2 pathway gene set used in this study consisted of 42 genes from the 'apoptosis and survival anti-apoptotic TNFs/NF- κ B/Bcl-2 pathway SuperPath' in the PathCards pathway unification database (Version 4.6.0.37, Weizmann Institute of Science). The p53 pathway gene set used in this study consisted of 132 genes from the 'p53 pathway (RnD) SuperPath' in the PathCards pathway unification database.

Plasmid construction and lentiviral transduction

The Coding Sequence (CDS) of the *firefly luciferase* gene was obtained by PCR amplification from the pGL3-Basic plasmid and inserted into the pCDH cDNA cloning and expression lentivector. Primers for the *firefly luciferase* CDS amplification were as follows: forward primer 5'-ATGGAAGACGCCAAAACATAAAG-3', reverse primer 5'-TTACACGGCGATCTTCCGCCCTT-3'. The pCDH plasmid was co-transfected with the pMD.2G and psPAX2 plasmids into 293FT cells to generate a *firefly luciferase* overexpression lentivirus. The lentivirus was subsequently added to the culture medium of Raji32 cells for 48 h of incubation. All the cells transfected with the lentivirus in this study were sorted based on green fluorescent protein using a MoFlo XDP instrument (Beckman Coulter, Brea, CA) and were termed Raji32-Luc cells.

Xenograft model

The 8-week-old female SCID (severe combined immunodeficiency) mice were purchased from SLAC

Laboratory Animal Co. (Shanghai, China). Raji32-Luc cells were resuspended in PBS and then injected intraperitoneally at 1.5×10^7 cells per mouse. The mice were divided into 4 groups (7 mice per group) based on the administered drugs, i.e., saline, rituximab, midostaurin and rituximab plus midostaurin. Rituximab was intraperitoneally injected at 118.4 mg/kg on days 8, 12 and 16, and midostaurin was administered by gavage at 20 mg/kg on days 8, 9, 10, 11, 12, 13, 14, 15, 16, 17, 18, 19, 20 and 21 after implantation. Saline was administered in the same way as rituximab with the same injection volume. Tumor growth was monitored by bioluminescence at 50, 70 and 90 days after implantation. For the in vivo luminescence imaging, D-luciferin (Promega, Madison, WI) was intraperitoneally injected (150 mg/kg). After 10 min, the mice were anesthetized by intraperitoneal injection with pentobarbital (50 mg/kg), and bioluminescence was then visualized using an In-Vivo MS FX PRO system (Bruker, Billerica, MA). The survival time of each mouse was recorded until 120 days. All the animal experiments were conducted in strict accordance with experimental protocols approved by the Animal Ethics Committee at Shanghai Medical School, Fudan University.

Statistics

The data are presented as the mean \pm SD unless otherwise specified. The significance of differences between two groups was determined using the two-tailed Student's *t*-test for unpaired data. For the total photon flux in the animal models, the significance of differences was determined using the one-tailed Mann-Whitney test. We applied the Mantel-Cox test to compare the survival rates of two groups of xenograft mouse models. In all analyses, $P < 0.05$ was considered statistically significant.

Results

Reduced CD20 and elevated CD59 expression levels led to the resistance of BL cells to rituximab-mediated CDC

The intrinsic features of immune cells precipitate the resistance to rituximab-mediated ADCC²⁰, while apoptosis plays a negligible role in rituximab antitumor activity. Therefore, we generated two BL cell lines, Ramos640 and Raji32, that were resistant to rituximab-mediated CDC at rituximab concentrations of 640 and 32 μ g/mL, respectively. Using immunoblotting (Fig. 1a, c) and FACS (Fig. 1b, d) assays, we found that CD20 expression decreased while CD59 expression increased in both resistant cell lines compared to the expression levels in the corresponding original cells (Fig. 1). However, the expression levels of two other mCRPs were not consistent between the two resistant cell lines. CD55 expression was reduced in Ramos640 cells but was increased in Raji32 cells, and CD46 expression was unchanged in Ramos640 cells but was reduced in Raji32 cells (Fig. 1). These results

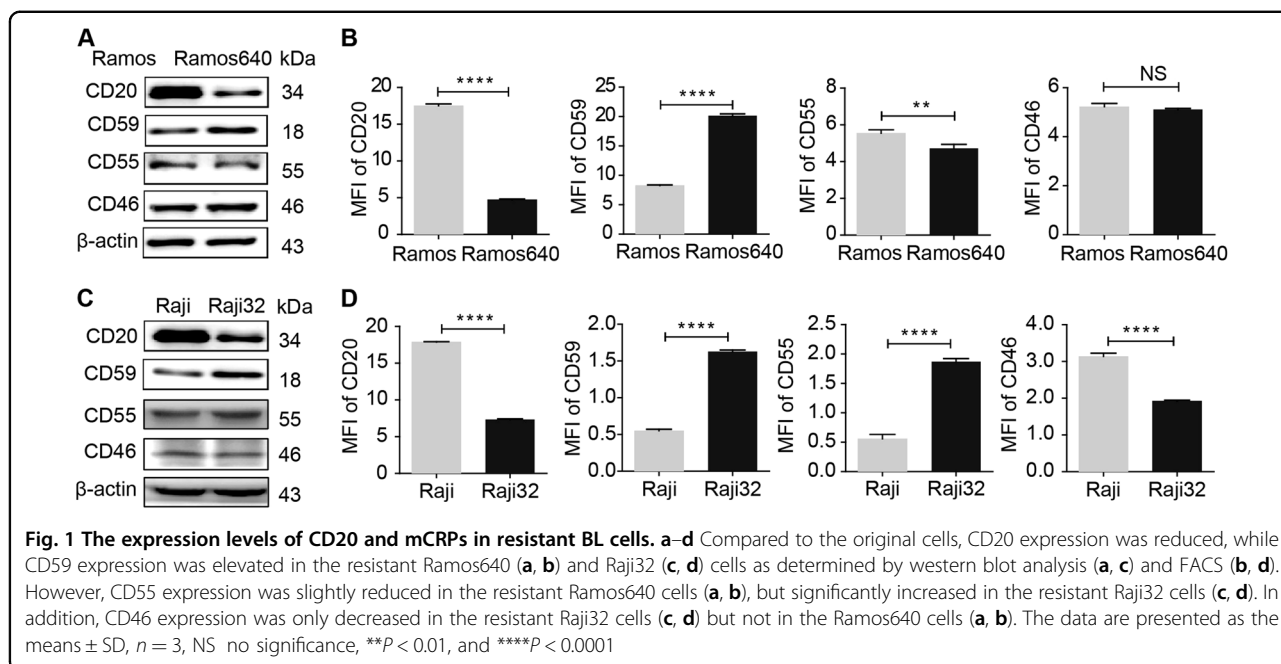


Table 1 Enriched pathways in Ramos640 vs Ramos cells based on an antibody microarray for profiling phosphorylation

KEGG pathway	P value	Fold enrichment	Count	Genes
hsa04151: PI3K-Akt signaling pathway	2.47E-15	18.60	13	CDKN1A, PTK2, CDKN1B, BCL2, CREB1, TP53, BAD, BCL2L1, ITGB3, PTEN, MYC, CHUK, AKT2
hsa05200: Pathways in cancer	1.24E-12	15.07	12	CDKN1A, PTK2, CDKN1B, JUN, BCL2, TP53, BAD, BCL2L1, PTEN, MYC, CHUK, AKT2
hsa04012: ErbB signaling pathway	5.35E-09	39.71	7	CDKN1A, PTK2, CDKN1B, JUN, BAD, MYC, AKT2
hsa05169: Epstein-Barr virus infection	1.59E-08	20.78	8	CDKN1A, CDKN1B, JUN, BCL2, TP53, MYC, CHUK, AKT2
hsa04210: Apoptosis	6.01E-08	47.76	6	BCL2, TP53, BAD, BCL2L1, CHUK, AKT2
hsa04510: Focal adhesion	9.41E-07	16.77	7	PTK2, JUN, BCL2, BAD, ITGB3, PTEN, AKT2
hsa05206: microRNAs in cancer	6.28E-06	12.12	7	CDKN1A, CDKN1B, BCL2, TP53, ITGB3, PTEN, MYC
hsa05202: Transcriptional misregulation in cancer	8.80E-06	17.63	6	CDKN1A, PTK2, CDKN1B, TP53, BCL2L1, MYC
hsa05205: Proteoglycans in cancer	2.06E-05	14.81	6	CDKN1A, PTK2, TP53, ITGB3, MYC, AKT2
hsa05203: Viral carcinogenesis	2.32E-05	14.45	6	CDKN1A, CDKN1B, JUN, CREB1, TP53, BAD

are consistent with previous reports showing that reduced CD20 and elevated CD59 levels contribute to the development of resistance to rituximab-mediated CDC^{17,21,22}. Considerable efforts have been made to improve rituximab therapeutic efficacy by increasing CD20 expression, for example, by administering the histone deacetylase inhibitor trichostatin A³⁷ or synthetic CpG oligodeoxynucleotides³⁸ or by inhibiting CD59 function with a modified monoclonal antibody^{39,40} or the bacterial toxin-derived ILYd4³². However, among these approaches, only CpG oligodeoxynucleotides were further evaluated in a

clinical trial (phase I) to determine their safety in B-cell non-Hodgkin lymphoma (NHL) patients⁴¹, and no further clinical trials have been reported. Therefore, alternative therapeutic strategies are still required.

PI3K/Akt pathway was strongly enriched in the resistant cells, but its inhibition failed to reverse the resistance

Considering the negligible effect of rituximab on inducing apoptosis in B-NHL, addition of a pro-apoptotic agent to rituximab therapy would be an ideal strategy. Therefore, an antibody microarray for phosphorylation

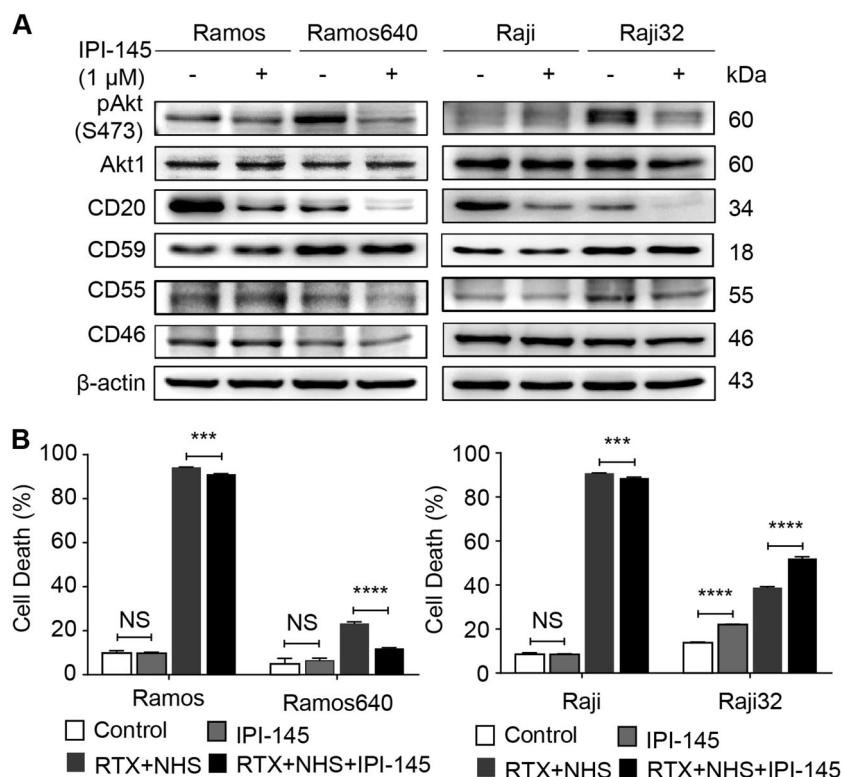


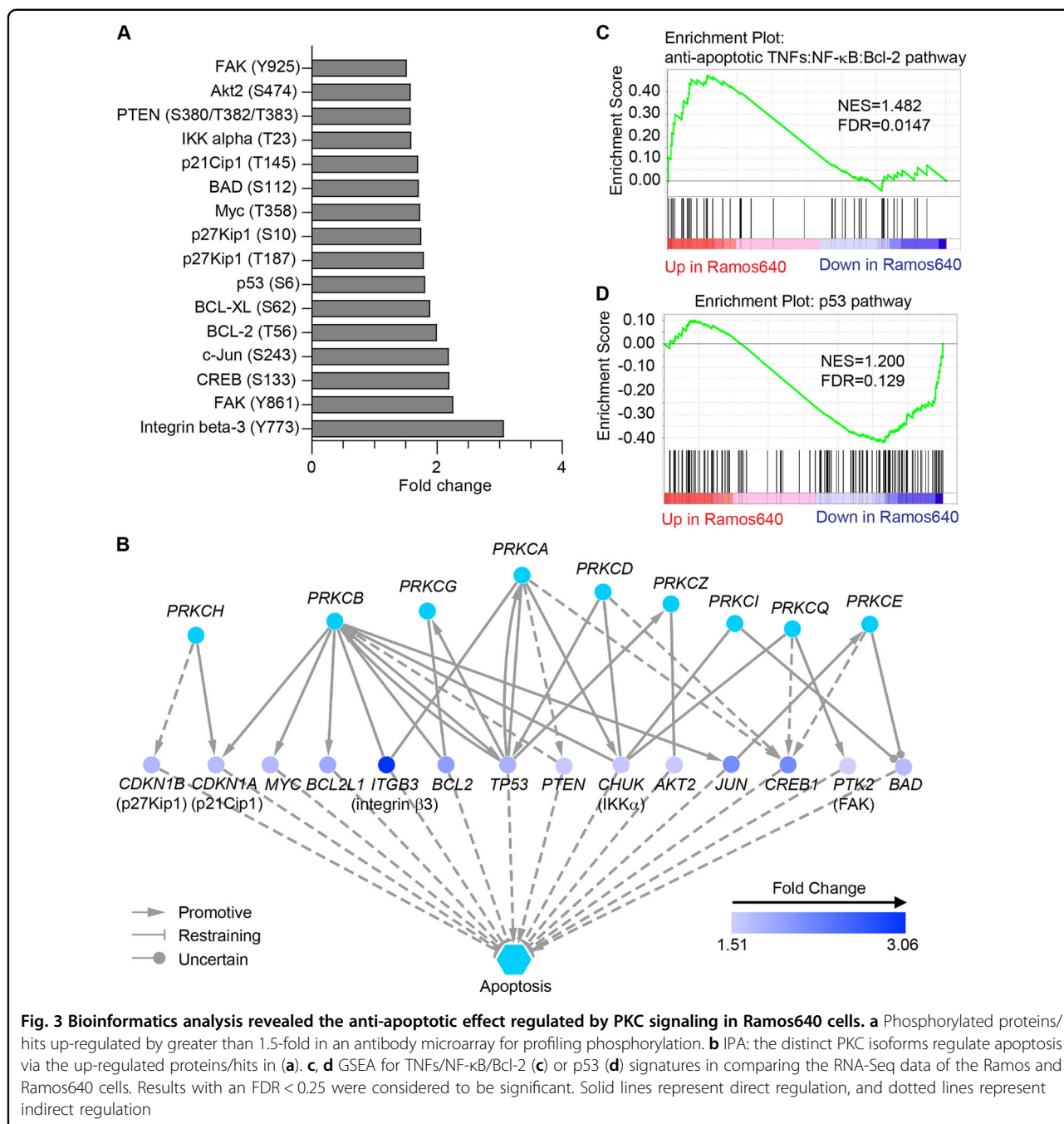
Fig. 2 PI3K/Akt inhibition failed to enhance the susceptibility of BL cells to rituximab-mediated CDC. **a** The phosphorylation levels of Akt (S473) increased in the resistant Ramos640 and Raji cells compared to the corresponding original cells, which could be suppressed by treatment with the PI3K inhibitor IPI-145, leading to reduced expression of CD20 and CD55. **b** The effect of combining IPI-145 with rituximab on rituximab-mediated CDC. IPI-145 alone failed to increase cell death in all the original and resistant cells except for the Raji32 cells. The addition of IPI-145 to rituximab also failed to increase rituximab-mediated CDC in the Ramos and Raji cells, but not in the Raji32 cells. In contrast, this combination treatment significantly increased rituximab-mediated CDC in the Raji32 cells. The data are represented as the means \pm SD, $n = 3$, NS no significance, $***P < 0.001$, $****P < 0.0001$. RTX rituximab, NHS normal human serum

profiling was used to identify the functional proteins and signaling pathways activated in Ramos640 cells. Fluorescence analysis revealed that the phosphorylation levels of 35 proteins were up- (31/35) or down-regulated (4/35) by greater than 1.4-fold in Ramos640 cells compared to the levels in Ramos cells (Supplementary Data 1). KEGG (Kyoto Encyclopedia of Genes and Genomes) signaling pathway analysis of these proteins demonstrated that PI3K/AKT signaling pathway contained the most phosphorylated proteins/hits, with 13, while apoptosis pathway displayed the greatest fold enrichment, at 47.76 (Table 1). Next, the PI3K inhibitor IPI-145 was used to determine whether PI3K inhibition could increase the susceptibility of resistant BL cells to rituximab treatment. We first confirmed that PI3K/Akt was activated in Ramos640 and Raji32 cells compared to the corresponding original cells and that IPI-145 effectively impaired the phosphorylation of Akt (Fig. 2a). However, CD20 expression was strongly suppressed by IPI-145 treatment in both original and resistant cells, whereas the expression levels of three mCRPs CD59, CD55 and CD46 were nearly unchanged

(Fig. 2a). These outcomes subsequently resulted in no effect or even a slightly negative effect of IPI-145 on the enhancement of rituximab-mediated CDC in the original and resistant cells, with the exception of Raji32 cells (Fig. 2b). In the Raji32 cells, IPI-145 alone or in combination with rituximab slightly enhanced cell death compared to that observed in the control or rituximab alone treatments, respectively (Fig. 2b, right panel). These results suggest that PI3K/Akt might not be a valuable drug target for facilitating rituximab treatment.

The PKC-mediated apoptosis pathway was highly activated in resistant cells

Although apoptosis pathway was identified as the most enriched in the antibody microarray, only six proteins were included in this pathway (Table 1), which hindered the isolation of the pathway modulators. Therefore, we narrowed the scope of the investigation by elevating the fold change of up- and down-regulated phosphorylated proteins/sites to 1.5 in the phosphorylation-profiling antibody microarray. The results revealed that a total of



16 proteins/sites were up-regulated by greater than 1.5-fold (Fig. 3a, and Supplementary Data 1). Notably, all of these up-regulated proteins/sites were determined to be involved in apoptosis according to the IPA (Fig. 3b). More importantly, the IPA also revealed that PKC signaling regulates all of these up-regulated proteins (Fig. 3b), although the detection of PKC phosphorylation was not included in the antibody microarray set used to profile phosphorylation. Using RNA-seq assay, we further found that the expression of genes in TNFs/NF-κB/2

pathway was strongly elevated, while the expression of genes in p53 pathway was significantly reduced in Ramos640 cells compared to the levels in Ramos cells based on the GSEA (Fig. 3c, d, and Supplementary Data 2). This analysis also indicated that the anti-apoptotic genes were up-regulated, while the pro-apoptotic genes were down-regulated. Therefore, these data suggested that PKC phosphorylated multiple downstream proteins, leading to the anti-apoptotic effect in Ramos640 cells.

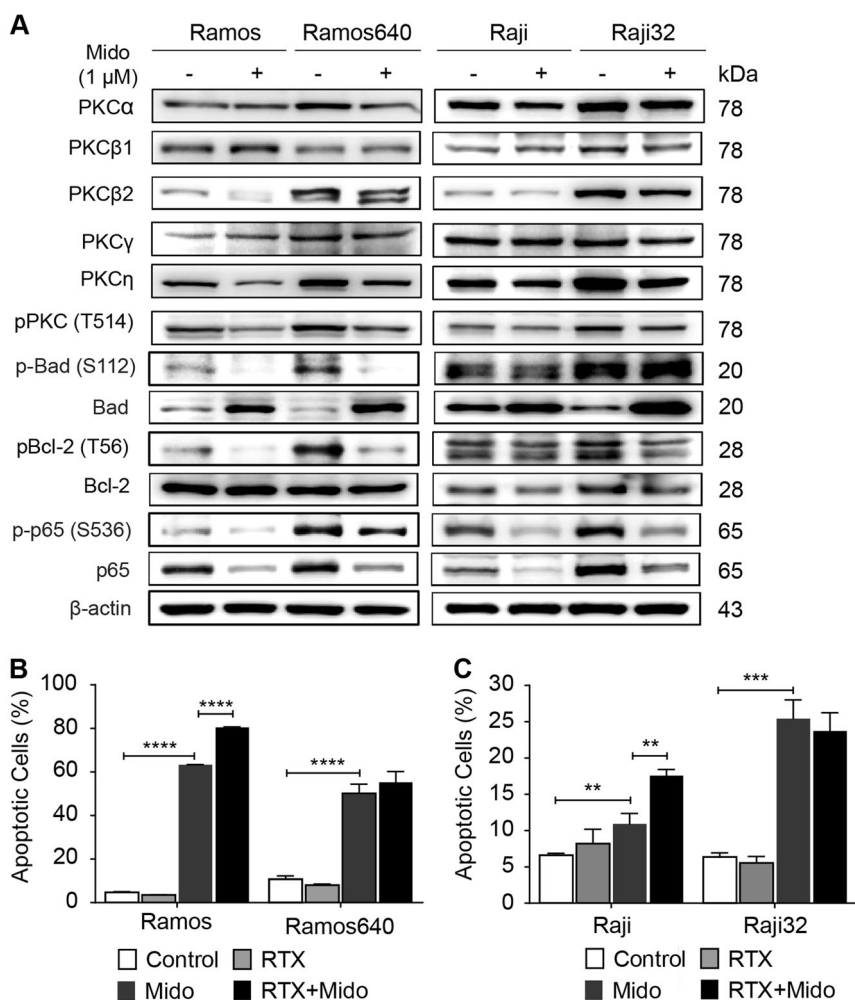


Fig. 4 PKC inhibition strongly induced apoptosis in both the original and resistant BL cells. **a** The indicated PKC isoforms were up-regulated in the resistant BL cells, leading to elevated levels of PKC phosphorylation and the activation of downstream anti-apoptotic proteins. **b, c** The pan-PKC inhibitor midostaurin potently induced apoptosis in the original and resistant Ramos (**b**) and Raji (**c**) cells, and the addition of rituximab to midostaurin significantly enhanced the pro-apoptotic effect in the Ramos640 cells. The data are presented as the means \pm SD, $n = 3$, ** $P < 0.01$, *** $P < 0.001$, **** $P < 0.0001$. RTX rituximab (640 or 32 μ g/mL for Ramos or Raji, respectively), Mido midostaurin (1 μ M)

The pan-PKC inhibitor midostaurin strongly promoted apoptosis

We compared the expression levels of five PKC isoforms in the original and resistant BL cells, and found that PKC α / β 2/ γ / η in Ramos640 and PKC α / β 1/ β 2/ η in Raji32 cells were overexpressed compared to the levels in the corresponding original cells. More importantly, the phosphorylation levels of PKC, which were detected by the sole commercially available antibody recognizing all PKC isoforms, were increased in both resistant cell lines (Fig. 4a). Further, we detected the efficacy of midostaurin in regulating PKC phosphorylation. Midostaurin is a multi-kinase inhibitor that was initially targeted toward PKC and is currently approved for acute myelogenous leukemia (AML) with an Fms-like tyrosine kinase 3 (FLT3) mutation and advanced systemic mastocytosis

(SM)^{42,43}. We observed that midostaurin suppressed the phosphorylation levels of PKC in both resistant BL cell lines and original Ramos cells but not original Raji cells and that this kinase inhibitor reduced the expression levels of PKC β 2/ η in Ramos cells, of PKC α / η in Ramos640 cells and of PKC β 1/ η in Raji32 cells (Fig. 4a).

Next, we verified the phosphorylation levels of several PKC downstream signaling molecules, including Bad, Bcl-2 and NF- κ B subunit p65. We first found that the phosphorylated levels of these molecules were significantly elevated (Fig. 4a). Furthermore, the expression levels of Bad were decreased, while those of p65 were increased in both resistant cell lines (Fig. 4a). All of the above changes may contribute to anti-apoptosis to a considerable degree, thus leading to the development of rituximab resistance in Ramos640 and Raji32 cells. In addition, midostaurin

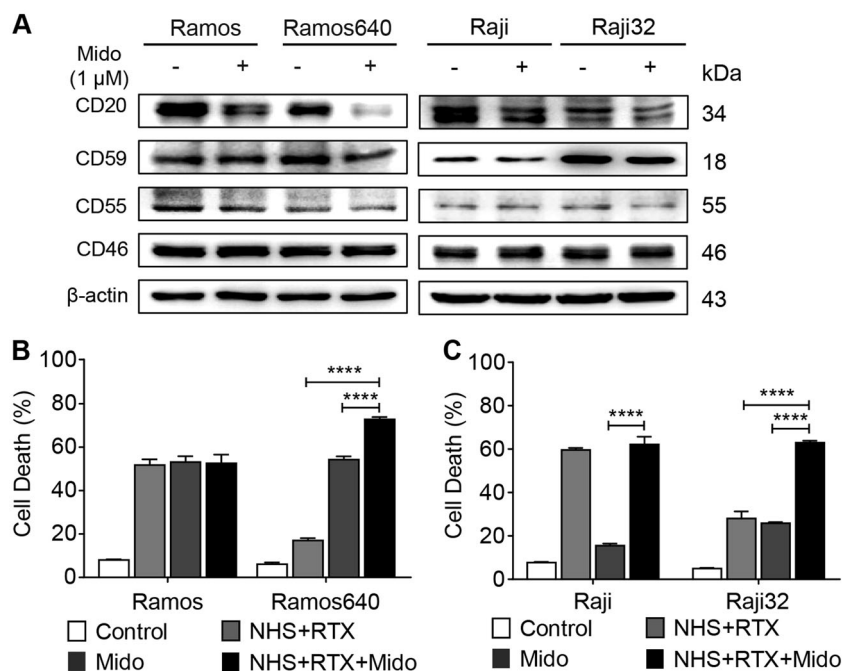


Fig. 5 Midostaurin additively enhanced rituximab-mediated CDC in resistant BL cells. **a** The PKC inhibitor significantly reduced CD20 expression in both the original and resistant cells and CD59 expression mainly in the resistant cells but did not alter the expression of CD55 or CD46 in the original or resistant cells. **b, c** The effect of the PKC inhibitor on rituximab-mediated CDC. The addition of the PKC inhibitor failed to enhance rituximab-mediated CDC in the original Ramos (**b**) and Raji (**c**) cells; however, the inhibitor additively enhanced CDC in the resistant Ramos640 (**b**) and Raji32 (**c**) cells. The data are presented as the means \pm SD, $n = 3$, **** $P < 0.0001$. RTX rituximab (40 or 4 μ g/mL for Ramos or Raji, respectively; or 640 or 32 μ g/mL for Ramos640 or Raji32, respectively), NHS normal human serum (20%), Mido midostaurin (1 μ M)

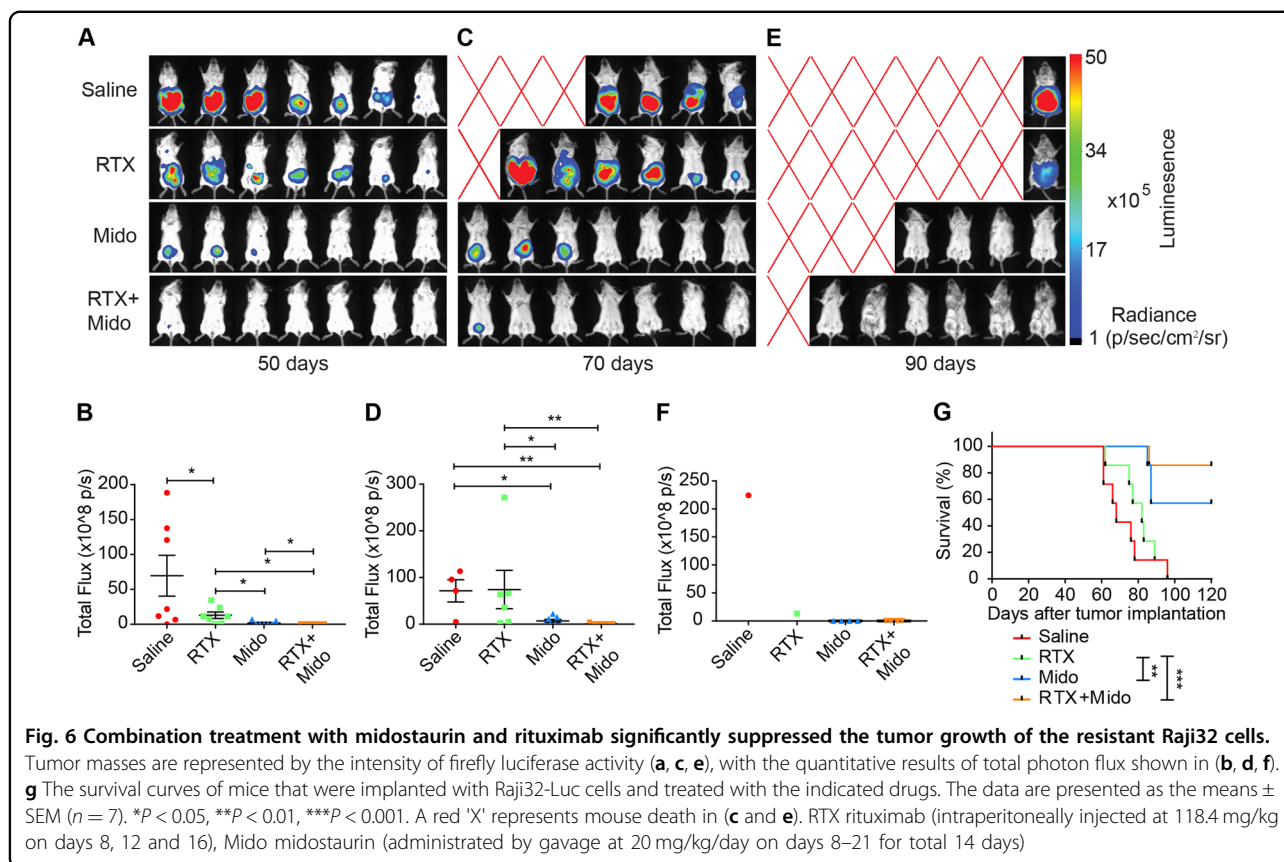
suppressed the phosphorylation levels of Bad, Bcl-2 and p65 in all the original and resistant cells (Fig. 4a). Moreover, midostaurin increased or reduced the expression of Bad or p65, respectively, in all four original and resistant cell lines and reduced the expression of Bcl-2 only in the original and resistant Raji cells (Fig. 4a). Therefore, midostaurin inhibited PKC and its subsequent downstream signaling molecules, which may lead to the pro-apoptotic effect in both Ramos and Raji cells to varying degrees. Among the cell lines, Raji cells appeared to be more resistant to midostaurin-mediated PKC inhibition than Ramos cells because midostaurin failed to suppress PKC phosphorylation.

Furthermore, we assessed the pro-apoptotic effects of midostaurin alone or in combination with rituximab on the original and resistant BL cells. As we expected, treatment with rituximab alone failed to induce apoptosis in all four original or resistant BL cell lines (Fig. 4b, c). However, compared to the culture medium control, midostaurin alone dramatically induced cell apoptosis in Ramos (from 4.7 to 63.3%), Ramos640 (from 10.8 to 50.2%) and Raji32 (from 6.4 to 25.4%) cells and slightly increased apoptosis (from 6.6% to 10.9%) in Raji cells, although the P value did reach statistical significance ($P = 0.0038$) (Fig. 4b, c). These results also functionally

indicated that, in general, Raji cells were more resistant to midostaurin-induced apoptosis than Ramos cells. In addition, the combination of midostaurin with rituximab resulted in slight pro-apoptotic effects only in the original but not in the resistant Ramos and Raji cell lines (Fig. 4b, c), further supporting the conclusion that rituximab induces a negligible pro-apoptotic effect, if any.

Midostaurin additively enhanced the susceptibility of resistant BL cells to rituximab-mediated CDC

Rituximab-mediated CDC can be regulated by the expression of mCRPs, such as CD46, CD55 and especially CD59, in addition to CD20^{17,22,44}. We observed that midostaurin reduced the expression levels of CD20 in all four BL cell lines and the levels of CD59 mainly in the resistant cells, while this inhibitor had no effect on the expression levels of CD55 or CD46 (Fig. 5a). These results suggested that midostaurin may hinder rituximab-mediated CDC due to the reduced expression of only CD20 in the original BL cells, while the effect of midostaurin on the resistant BL cells requires further examination due to the reduced expression of both CD20 and CD59. In addition, these results revealed a difference between the IPI-145 and midostaurin effects on regulating CD20 and CD59 expression, in which IPI-145 only



reduced CD20 but not CD59 expression in the resistant BL cells (Fig. 2a).

While rituximab plus NHS potently induced CDC in the original Ramos and Raji cells, addition of midostaurin failed to enhance the susceptibility to rituximab-mediated CDC, although midostaurin promoted apoptosis (Fig. 5b, c). This result may be caused by the reduced CD20 expression and the already high cell death rate induced by treatment with rituximab alone. In contrast, addition of rituximab significantly enhanced the cytotoxic effect of midostaurin in both original BL cell lines (Fig. 5b, c), indicating that rituximab-mediated CDC dominated over midostaurin-induced apoptosis in the original BL cells. Notably, we found that the cytotoxic effect of the combined rituximab and midostaurin treatment appeared to be additive in the resistant Ramos640 and Raji32 cells. Rituximab and midostaurin induced 17.1 and 54.3% cell death, respectively, while the combination induced 72.8% cell death (Fig. 5b). Similarly, rituximab and midostaurin induced 28.0 and 25.8% cell death, respectively, while their combination induced 62.9% cell death (Fig. 5c). These results may be due to the distinct antitumor mechanisms of rituximab and midostaurin.

Combination treatment of rituximab with midostaurin significantly suppressed tumor growth of the resistant cells

Given that the potent pro-apoptotic effect of midostaurin may help increase rituximab antitumor activity, we tested the efficacy of a combination treatment of rituximab with midostaurin in immunodeficient mice that were implanted with the more resistant Raji32 cells transfected with a luciferase-expressing plasmid. On day 50 after implantation, the tumor growth represented by total flux was ranked in the order of saline, rituximab, midostaurin and rituximab plus midostaurin, in which all the adjacent groups exhibited statistically significant differences in tumor mass (Fig. 6a, b). On day 70, 3 out of 7 mice died in the saline group, 1 out of 7 died in the rituximab group, and all 7 mice survived in the midostaurin and combination treatment groups (Fig. 6c). The tumor mass in the surviving mice showed consistent results (Fig. 6d). On day 90, 1 out of 7, 4 out of 7, or 6 out of 7 mice survived in the saline or rituximab groups, midostaurin group, or combination treatment group, respectively (Fig. 6e). The tumor mass in the surviving mouse with saline treatment was greater than that in the

surviving mouse with rituximab treatment (Fig. 6f). In addition, the survival curve analysis demonstrated that compared to rituximab alone, midostaurin alone or in combination with rituximab significantly prolonged the survival rate (Fig. 6g), indicating that the pro-apoptotic effect induced by midostaurin may be a necessary and beneficial supplement to the therapeutic regimen, especially for the treatment of resistant BL.

Discussion

In the present study, we revealed that PKC was highly up-regulated and activated in rituximab-resistant BL cells. The administration of the pan-PKC inhibitor midostaurin alone or in combination with rituximab potently elicited apoptosis and dramatically improved OS, especially in resistant BL cells. Although the function of PKC in cancer development remains controversial⁴⁵, PKC inhibitors are being widely tested for the treatment of multiple types of cancer in clinical trials. In April 2017, midostaurin was approved for the treatment of AML with the FLT3 mutation and advanced SM^{42,43,46}. Currently, no clinical trials for BL treatment are registered at clinicaltrials.gov, although there have been a small number of studies reporting the importance of PKC activation in BL cells^{47,48}. Therefore, our findings suggest that it is imperative to perform a clinical trial of midostaurin alone or in combination with rituximab, preferably for relapsed/refractory BL patients and possibly for other relapsed/refractory NHL patients with highly activated PKC.

Rituximab has achieved great success in the treatment of a broad variety of B-cell lymphomas. Rituximab may destroy CD20-expressing lymphocytes mainly via ADCC and CDC by binding to the CD20 on the membrane^{17–19}. However, resistance to rituximab remains a major challenge for relapsed/refractory patients. Approximately 50% of patients are unresponsive to rituximab treatment despite CD20 expression, and initially responsive patients eventually develop resistance to further rituximab treatment^{17,18}. It may be not possible to overcome the resistance to ADCC because this resistance likely results from the intrinsic immune features of patients²⁰. Therefore, the current approaches mainly focus on enhancing the efficacy of rituximab-mediated CDC, including up-regulating CD20 expression using the histone deacetylase inhibitor trichostatin A³⁷ or synthetic CpG oligodeoxynucleotides³⁸ and inhibiting CD59 function using a modified monoclonal antibody^{39,40} or a bacterial toxin-derived ILYd4³². However, these effects observed in experimental systems require further careful investigation, including an assessment of their toxicity.

Although a direct rituximab-induced cytotoxic effect on lymphocytes is somewhat controversial, numerous studies in various NHL cells have demonstrated that rituximab lacks pro-apoptotic capability. Some strategies have been

implemented to sensitize rituximab therapy by combining with other agents to increase the pro-apoptotic effect. These additional agents include macromolecules such as the humanized monoclonal mapatumumab targeting TRAIL-R1⁴⁹, the genetically engineered fusion proteins scFvRit:sFasL⁵⁰, Apo2 ligand (Apo2L)/TRAIL (dulacinermin)^{51,52} and anti-CD20-interleukin-21⁵³, and small molecules, such as the selective NEDD8 activating enzyme inhibitor pevonedistat (MLN4924)⁵⁴, the mTOR (mammalian target of rapamycin) inhibitor temsirinolimuz⁵⁵, and the proteasome inhibitor bortezomib⁵⁶. However, the efficacy of these agents requires further confirmation or has been suggested to be insufficient based on clinical trials⁵². Interestingly, obinutuzumab (GA101), a novel type II glycol-engineered humanized monoclonal anti-CD20 IgG1 antibody, has shown its superior efficacy against CLL (chronic lymphocytic leukemia) and relapsed/refractory indolent NHL to rituximab^{57,58}, due to the enhanced capability of inducing direct cell death and ADCC, though less potent in mediating CDC⁵⁹. Moreover, the similar superior efficacy of obinutuzumab to rituximab has also been observed in rituximab-sensitive/resistant BL^{60,61}. Although the underlying mechanisms by which obinutuzumab is able to induce strong direct cell death remain largely obscure, several mediators have been suspected including reactive oxygen species²⁷, BCR (B cell antigen receptor) or cytotoxicity pathway⁶¹. Therefore, whether addition of midostaurin to obinutuzumab could enhance the antitumor activity is worthy of future investigation. Herein, we reported that midostaurin strongly enhanced rituximab activity by promoting apoptosis via PKC inhibition in BL cells.

Midostaurin was modified from staurosporine to improve the selectivity toward PKC and was then further found to inhibit other kinases, such as FLT3, PDGFR, KIT and VEGFR2, together with the midostaurin metabolites⁶². Midostaurin was found to be safe and tolerable when administered as a chronic oral therapy in a phase I clinical trial⁶³ and was approved by the FDA (Food and Drug Administration) based on its effectiveness⁶⁴. Considering that PKC was highly phosphorylated in the resistant BL cells, we tested the in vitro and in vivo effects of midostaurin on potentiating rituximab antitumor activity in the original and resistant BL cells. We found that midostaurin strongly enhanced rituximab cytotoxicity, especially in the resistant BL cells, by promoting apoptosis, possibly by altering the phosphorylation of downstream signaling molecules, including Bad, Bcl-2 and NF- κ B. Our findings support the further evaluation in clinical trials of midostaurin alone or in combination with rituximab and with or without short-term intensive chemotherapy in relapsed/refractory BL patients.

Acknowledgements

This work was supported by grants to X.G. from the National Natural Science Foundation of China (81402570) and to W.H. from the National Natural Science Foundation of China (81372258) and by a grant to W.H. from the Shanghai Science and Technology Committee (16JC1405500). The RNA-seq data of the Ramos and Ramos640 cells were deposited into the National Center for Biotechnology Information Gene Expression Omnibus database (GSE112592).

Conflict of interest

The authors declare that they have no conflict of interest.

Publisher's note

Springer Nature remains neutral with regard to jurisdictional claims in published maps and institutional affiliations.

Supplementary Information accompanies this paper at (<https://doi.org/10.1038/s41419-018-1259-5>).

Received: 29 September 2018 Accepted: 3 December 2018

Published online: 18 December 2018

References

- Bishop, P. C., Rao, V. K. & Wilson, W. H. Burkitt's lymphoma: molecular pathogenesis and treatment. *Cancer Invest.* **18**, 574–583 (2000).
- Longo, D. L. et al. Diffuse small noncleaved-cell, non-Burkitt's lymphoma in adults: a high-grade lymphoma responsive to ProMACE-based combination chemotherapy. *J. Clin. Oncol.* **12**, 2153–2159 (1994).
- Jost, L. M. et al. Short-term weekly chemotherapy followed by high-dose therapy with autologous bone marrow transplantation for lymphoblastic and Burkitt's lymphomas in adult patients. *Ann. Oncol.* **6**, 445–451 (1995).
- Cairo, M. S. et al. Results of a randomized international study of high-risk central nervous system B non-Hodgkin lymphoma and B acute lymphoblastic leukemia in children and adolescents. *Blood* **109**, 2736–2743 (2007).
- Patte, C. et al. Results of the randomized international FAB/LMB96 trial for intermediate risk B-cell non-Hodgkin lymphoma in children and adolescents: it is possible to reduce treatment for the early responding patients. *Blood* **109**, 2773–2780 (2007).
- Lee, E. J. et al. Brief-duration high-intensity chemotherapy for patients with small noncleaved-cell lymphoma or FAB L3 acute lymphocytic leukemia: results of cancer and leukemia group B study 9251. *J. Clin. Oncol.* **19**, 4014–4022 (2001).
- Divine, M. et al. Burkitt lymphoma in adults: a prospective study of 72 patients treated with an adapted pediatric LMB protocol. *Ann. Oncol.* **16**, 1928–1935 (2005).
- Mead, G. M. et al. An international evaluation of CODOX-M and CODOX-M alternating with IVAC in adult Burkitt's lymphoma: results of United Kingdom Lymphoma Group LY06 study. *Ann. Oncol.* **13**, 1264–1274 (2002).
- Mead, G. M. et al. A prospective clinicopathologic study of dose-modified CODOX-M/IVAC in patients with sporadic Burkitt lymphoma defined using cytogenetic and immunophenotypic criteria (MRC/NCRI LY10 trial). *Blood* **112**, 2248–2260 (2008).
- Coiffier, B. et al. CHOP chemotherapy plus rituximab compared with CHOP alone in elderly patients with diffuse large-B-cell lymphoma. *N. Engl. J. Med.* **346**, 235–242 (2002).
- Barnes, J. A. et al. Evaluation of the addition of rituximab to CODOX-M/IVAC for Burkitt's lymphoma: a retrospective analysis. *Ann. Oncol.* **22**, 1859–1864 (2011).
- Corazzelli, G. et al. RD-CODOX-M/IVAC with rituximab and intrathecal liposomal cytarabine in adult Burkitt lymphoma and 'unclassifiable' highly aggressive B-cell lymphoma. *Br. J. Haematol.* **156**, 234–244 (2012).
- Rizzieri, D. A. et al. Improved efficacy using rituximab and brief duration, high intensity chemotherapy with filgrastim support for Burkitt or aggressive lymphomas: cancer and Leukemia Group B study 10 002. *Br. J. Haematol.* **165**, 102–111 (2014).
- Wasterlid, T. et al. Impact of chemotherapy regimen and rituximab in adult Burkitt lymphoma: a retrospective population-based study from the Nordic Lymphoma Group. *Ann. Oncol.* **24**, 1879–1886 (2013).
- Goldman, S. et al. Rituximab with chemotherapy in children and adolescents with central nervous system and/or bone marrow-positive Burkitt lymphoma/leukaemia: a Children's Oncology Group Report. *Br. J. Haematol.* **167**, 394–401 (2014).
- Ribrag, V. et al. Rituximab and dose-dense chemotherapy for adults with Burkitt's lymphoma: a randomised, controlled, open-label, phase 3 trial. *Lancet* **387**, 2402–2411 (2016).
- Zhou, X., Hu, W. & Qin, X. The role of complement in the mechanism of action of rituximab for B-cell lymphoma: implications for therapy. *Oncologist* **13**, 954–966 (2008).
- Smith, M. R. Rituximab (monoclonal anti-CD20 antibody): mechanisms of action and resistance. *Oncogene* **22**, 7359–7368 (2003).
- Weiner, G. J. Rituximab: mechanism of action. *Semin. Hematol.* **47**, 115–123 (2010).
- Cartron, G. et al. Therapeutic activity of humanized anti-CD20 monoclonal antibody and polymorphism in IgG Fc receptor Fcγ3 gene. *Blood* **99**, 754–758 (2002).
- Manches, O. et al. In vitro mechanisms of action of rituximab on primary non-Hodgkin lymphomas. *Blood* **101**, 949–954 (2003).
- Fishelson, Z. Obstacles to cancer immunotherapy: expression of membrane complement regulatory proteins (mCRPs) in tumors. *Mol. Immunol.* **40**, 109–123 (2003).
- Clynes, R. A., Towers, T. L., Presta, L. G. & Ravetch, J. V. Inhibitory Fc receptors modulate in vivo cytotoxicity against tumor targets. *Nat. Med.* **6**, 443–446 (2000).
- Glennie, M. J., French, R. R., Cragg, M. S. & Taylor, R. P. Mechanisms of killing by anti-CD20 monoclonal antibodies. *Mol. Immunol.* **44**, 3823–3837 (2007).
- de Haij, S. et al. In vivo cytotoxicity of type I CD20 antibodies critically depends on Fc receptor ITAM signaling. *Cancer Res.* **70**, 3209–3217 (2010).
- Wilson, N. S. et al. An Fcγ3 receptor-dependent mechanism drives antibody-mediated target-receptor signaling in cancer cells. *Cancer Cell* **19**, 101–113 (2011).
- Honeychurch, J. et al. Antibody-induced nonapoptotic cell death in human lymphoma and leukemia cells is mediated through a novel reactive oxygen species-dependent pathway. *Blood* **119**, 3523–3533 (2012).
- Okroj, M., Osterborg, A. & Blom, A. M. Effector mechanisms of anti-CD20 monoclonal antibodies in B cell malignancies. *Cancer Treat. Rev.* **39**, 632–639 (2013).
- Taylor, R. P. & Lindorfer, M. A. The role of complement in mAb-based therapies of cancer. *Methods* **65**, 18–27 (2014).
- Montalva, F. et al. The mechanism of anti-CD20-mediated B cell depletion revealed by intravital imaging. *J. Clin. Invest.* **123**, 5098–5103 (2013).
- Winkler, D. G. et al. PI3K-δ and PI3K-γ inhibition by IPI-145 abrogates immune responses and suppresses activity in autoimmune and inflammatory disease models. *Chem. Biol.* **20**, 1364–1374 (2013).
- Hu, W. et al. Human CD59 inhibitor sensitizes rituximab-resistant lymphoma cells to complement-mediated cytolysis. *Cancer Res.* **71**, 2298–2307 (2011).
- Huang da, W., Sherman, B. T. & Lempicki, R. A. Systematic and integrative analysis of large gene lists using DAVID bioinformatics resources. *Nat. Protoc.* **4**, 44–57 (2009).
- Liu, Z. et al. Autism-like behaviours and germline transmission in transgenic monkeys overexpressing MeCP2. *Nature* **530**, 98–102 (2016).
- Mootha, V. K. et al. PGC-1α-responsive genes involved in oxidative phosphorylation are coordinately downregulated in human diabetes. *Nat. Genet.* **34**, 267–273 (2003).
- Subramanian, A. et al. Gene set enrichment analysis: a knowledge-based approach for interpreting genome-wide expression profiles. *Proc. Natl. Acad. Sci. USA* **102**, 15545–15550 (2005).
- Tomita, A. et al. Epigenetic regulation of CD20 protein expression in a novel B-cell lymphoma cell line, RRBL1, established from a patient treated repeatedly with rituximab-containing chemotherapy. *Int. J. Hematol.* **86**, 49–57 (2007).
- Jahrsdorfer, B. et al. B-cell lymphomas differ in their responsiveness to CpG oligodeoxynucleotides. *Clin. Cancer Res.* **11**, 1490–1499 (2005).
- Macor, P. et al. In vivo targeting of human neutralizing antibodies against CD55 and CD59 to lymphoma cells increases the antitumor activity of rituximab. *Cancer Res.* **67**, 10556–10563 (2007).
- Macor, P. et al. Bispecific antibodies targeting tumor-associated antigens and neutralizing complement regulators increase the efficacy of antibody-based immunotherapy in mice. *Leukemia* **29**, 406–414 (2015).
- Witzig, T. E. et al. A phase I trial of immunostimulatory CpG 7909 oligodeoxynucleotide and 90 yttrium ibritumomab tiuxetan radioimmunotherapy

- for relapsed B-cell non-Hodgkin lymphoma. *Am. J. Hematol.* **88**, 589–593 (2013).
42. Stone, R. M. et al. Midostaurin plus chemotherapy for acute myeloid leukemia with a FLT3 mutation. *N. Engl. J. Med.* **377**, 454–464 (2017).
 43. Gotlib, J. et al. Efficacy and safety of midostaurin in advanced systemic mastocytosis. *N. Engl. J. Med.* **374**, 2530–2541 (2016).
 44. Golay, J. et al. CD20 levels determine the in vitro susceptibility to rituximab and complement of B-cell chronic lymphocytic leukemia: further regulation by CD55 and CD59. *Blood* **98**, 3383–3389 (2001).
 45. Isakov, N. Protein kinase C (PKC) isoforms in cancer, tumor promotion and tumor suppression. *Semin. Cancer Biol.* **48**, 36–52 (2018).
 46. Wei, A. H. & Tiong, I. S. Midostaurin, enasidenib, CPX-351, gemtuzumab ozogamicin, and venetoclax bring new hope to AML. *Blood* **130**, 2469–2474 (2017).
 47. Knox, K. A. et al. Second-messenger pathways involved in the regulation of survival in germinal-centre B cells and in Burkitt lymphoma lines. *Int. J. Cancer* **52**, 959–966 (1992).
 48. Keenan, C., Thompson, S., Knox, K. & Pears, C. Protein kinase C- α is essential for Ramos-BL B cell survival. *Cell. Immunol.* **196**, 104–109 (1999).
 49. Maddipati, S., Hernandez-Ilizaliturri, F. J., Knight, J. & Czuczman, M. S. Augmented antitumor activity against B-cell lymphoma by a combination of monoclonal antibodies targeting TRAIL-R1 and CD20. *Clin. Cancer Res.* **13**, 4556–4564 (2007).
 50. Bremer, E. et al. Superior activity of fusion protein scFvRitsFasL over cotreatment with rituximab and Fas agonists. *Cancer Res.* **68**, 597–604 (2008).
 51. Daniel, D. et al. Cooperation of the proapoptotic receptor agonist rhApo2L/TRAIL with the CD20 antibody rituximab against non-Hodgkin lymphoma xenografts. *Blood* **110**, 4037–4046 (2007).
 52. Cheah, C. Y. et al. Dulanermin with rituximab in patients with relapsed indolent B-cell lymphoma: an open-label phase 1b/2 randomised study. *Lancet Haematol.* **2**, e166–e174 (2015).
 53. Bhatt, S. et al. Anti-CD20-interleukin-21 fusokine targets malignant B cells via direct apoptosis and NK-cell-dependent cytotoxicity. *Blood* **129**, 2246–2256 (2017).
 54. Czuczman, N. M. et al. Pevonedistat, a NEDD8-activating enzyme inhibitor, is active in mantle cell lymphoma and enhances rituximab activity in vivo. *Blood* **127**, 1128–1137 (2016).
 55. Zoellner, A. K. et al. Temsirolimus acts as additive with bendamustine in aggressive lymphoma. *Ann. Hematol.* **95**, 403–407 (2016).
 56. Wang, M. et al. Bortezomib is synergistic with rituximab and cyclophosphamide in inducing apoptosis of mantle cell lymphoma cells in vitro and in vivo. *Leukemia* **22**, 179–185 (2008).
 57. Goede, V. et al. Obinutuzumab plus chlorambucil in patients with CLL and coexisting conditions. *N. Engl. J. Med.* **370**, 1101–1110 (2014).
 58. Gabellier, L. & Cartron, G. Obinutuzumab for relapsed or refractory indolent non-Hodgkin's lymphomas. *Ther. Adv. Hematol.* **7**, 85–93 (2016).
 59. Herter, S. et al. Preclinical activity of the type II CD20 antibody GA101 (obinutuzumab) compared with rituximab and ofatumumab in vitro and in xenograft models. *Mol. Cancer Ther.* **12**, 2031–2042 (2013).
 60. Awasthi, A. et al. Obinutuzumab (GA101) compared to rituximab significantly enhances cell death and antibody-dependent cytotoxicity and improves overall survival against CD20(+) rituximab-sensitive/-resistant Burkitt lymphoma (BL) and precursor B-acute lymphoblastic leukaemia (pre-B-ALL): potential targeted therapy in patients with poor risk CD20(+) BL and pre-B-ALL. *Br. J. Haematol.* **171**, 763–775 (2015).
 61. Awasthi, A. et al. A comparative global phosphoproteomics analysis of obinutuzumab (GA101) versus rituximab (RTX) against RTX sensitive and resistant Burkitt lymphoma (BL) demonstrates differential phosphorylation of signaling pathway proteins after treatment. *Oncotarget* **8**, 113895–113909 (2017).
 62. Stone, R. M., Manley, P. W., Larson, R. A. & Capdeville, R. Midostaurin: its odyssey from discovery to approval for treating acute myeloid leukemia and advanced systemic mastocytosis. *Blood Adv.* **2**, 444–453 (2018).
 63. Propper, D. J. et al. Phase I and pharmacokinetic study of PKC412, an inhibitor of protein kinase C. *J. Clin. Oncol.* **19**, 1485–1492 (2001).
 64. Kim, E. S. Midostaurin: first global approval. *Drugs* **77**, 1251–1259 (2017).